Proceedings of the 21st ICSMGE, Vienna, Austria, 14 – 19 June 2026. Pistrol, Adam & Schweiger (eds.)
Published by: ÖGG, Austrian Society for Geomechanics, Salzburg, Austria, ISBN 978-3-9503898-4-5
https://doi.org/10.53243/ICSMGE2026-1431

Effect of carbonation on the geo-mechanical behaviour of alkali-activated fine-grained soils

Elise Lefèvre, Pierre Gerard, Alessia Cuccurullo
Building, Architecture and Town Planning (BATir), Université Libre de Bruxelles, Belgium, elise.lefevre@ulb.be

Agostino Walter Bruno
Dipartimento di Ingegneria Civile, Chimica e Ambientale, Università degli Studi di Genova, Italy

ABSTRACT: The shift toward sustainable soil stabilization has renewed interest in using industrial and agricultural by-products as alternatives to conventional binders like Portland cement and lime. Alkali-activated binders, formed by reacting aluminosilicate-rich precursors with sodium or potassium activators, are promising alternatives due to their capacity to bond soil particles together, increasing both stiffness and strength of the material. However, concerns about CO_2 exposure effects on calcium-rich, alkali-activated materials have arisen. In these materials, carbon dioxide diffuses into soil pores and reacts with calcium to form calcium carbonate - a process known as carbonation. While well-studied in Portland cement and lime-stabilized soils, the impact of carbonation on the microstructure and hydro-mechanical behaviour of alkali-activated soils remains underexplored. The main aim of this study is therefore to investigate the kinetics of alkali-activation and carbonation reactions, focusing on micro- and macro-scale changes in partially saturated fine-grained soils (the most common condition for shallow stabilized soils). It examines how both natural carbonation and curing time influence the geo-mechanical behaviour of the material. To deepen the understanding of macro-scale observations and the assumptions drawn from unconfined compression tests, different multi-scale experimental techniques are employed, including X-ray diffraction and mercury intrusion porosimetry. These methods allow for the comparison of pore size distributions and the analysis of bonding phase development, providing valuable insights into the material's overall performance.

KEYWORDS: Soil stabilization, alkali-activated materials, carbonation.

1 INTRODUCTION

Soil stabilization is an essential process in geotechnical engineering, commonly applied in projects such as embankments, road foundations, and slope stabilization. It involves the physical and/or chemical modification of problematic and naturally weak soils, particularly those prone to shrinkage or swelling upon wetting and drying, with the objective of enhancing their mechanical and durability performances.

Traditional soil stabilization techniques, which typically rely on the addition of cement and/or lime, raise significant environmental concerns due to the energy-intensive manufacturing processes of these materials and their substantial CO_2 emissions (Mavroulidou et al., 2022). Cement production alone is responsible for approximately 7–8% of global CO_2 emissions (Li and Wu, 2022; Lamaa et al., 2023), while also emitting other harmful air pollutants such as sulfur dioxide, carbon monoxide, and nitrogen oxides (Mavroulidou et al., 2022).

In the context of global climate targets and the urgent need to reduce CO_2 emissions, the development of alternative and more sustainable soil stabilization methods has become a key objective in the field. Among the promising solutions, the alkali-activation of calcium-rich industrial by-products such as ground granulated blast furnace slag (GGBS) stands out for its potential to significantly reduce the environmental footprint of soil treatment (Tonini De Araújo et al., 2023). When combined with an alkaline activator, typically sodium hydroxide (NaOH), a chemical reaction is triggered that leads to the formation of amorphous aluminosilicate gels, primarily calcium-alumino-silicate-hydrate (C-A-S-H), and to a lesser extent, sodium-alumino-silicate-hydrate (N-A-S-H) or hybrid gels, depending on the system chemistry. These gel phases progressively polymerize to form a dense matrix, that improves the mechanical performance and durability of the treated soil (Vitale et al., 2017; Marsh et al., 2019a; Razeghi et al., 2024).

This type of binder system can reduce greenhouse gas emissions by up to 80% compared to traditional cement-based stabilization (Tonini De Araújo et al., 2023), particularly when incorporating waste-derived precursors such as GGBS, thereby supporting circular economy principles (Mavroulidou et al., 2022).

In recent years, studies on the geotechnical behaviour of alkali-activated soils have expanded significantly, reporting notable improvements in unconfined compressive strength and stiffness. These performances are strongly influenced by factors such as precursor type, activator concentration, curing conditions, and soil mineralogy (Cristelo et al., 2012; Mazhar et al., 2018; Marsh et al., 2019b; Murmu, Jain and Patel, 2019; Miraki et al., 2022). Despite these advantages, the long-term durability of GGBS-alkali-activated soils under environmental exposure remains insufficiently investigated, particularly with regard to carbonation. Carbonation occurs when atmospheric CO_2 diffuses into the pore network of the material, dissolves into the pore solution, and forms carbonic acid (H_2CO_3). This acid subsequently reacts with alkaline ions, particularly calcium ions (Ca^{2+}), to form stable carbonate phases, such as calcite or aragonite. In calcium-rich alkali-activated systems (GGBS alkali-activated systems), carbonation can occur both through the reaction of free or loosely bound calcium ions, mainly coming from the GGBS precursor, and through the leaching of calcium from the C-A-S-H gel itself, a process known as gel decalcification. This latter mechanism can compromise the integrity of the binding phase and affect long-term durability (Lamaa et al., 2023). Nonetheless, some studies suggest that carbonation may further enhance the strength of alkali-activated soils under specific conditions by promoting the formation of carbonate phases, contributing to matrix densification (Ko, Chen and Jiang, 2015; Polettini, Pomi and Stramazzo, 2016; Fasihnikoutalab Mohammad Hamed et al., 2017; Razeghi et al., 2024; Cui et al., 2025). However, most of these investigations have been conducted under accelerated carbonation conditions, involving elevated CO_2 pressures. In contrast, the effects of natural carbonation, more representative of field exposure, have received limited attention.

In this context, the present study aims to address this research gap by evaluating the impact of natural carbonation on the microstructural and mechanical evolution of GGBS alkali-

activated fine-grained soil. Stabilized soil samples were prepared and cured under sealed or naturally carbonating conditions for 7 and 28 days. Their unconfined compressive strength (UCS) was evaluated alongside complementary characterization techniques, including X-Ray diffraction (XRD) and mercury intrusion porosimetry (MIP), to assess changes in mineralogical phases and pore structure. This approach provides preliminary insights into the combined effects of alkali-activation and natural carbonation reactions on the behaviour of stabilized soils.

2 MATERIALS AND METHODS

2.1 *Materials*

The soil used in this study is a clayey silt collected from Marche-les-Dames (MLD) region in Belgium. The soil is composed of approximately 13% clay, 62% silt and 25% sand. Following ASTM D4318 (2017), the liquid limit (LL), plastic limit (PL) and plasticity index (PI) were determined as 28.4%, 19.6% and 8.8%, respectively, which classifies it as CL (low plasticity clay) according to the Unified Soil classification system. Moreover, the Standard Proctor compaction test, conducted in accordance with ASTM D698 (2021), indicated an optimum moisture content (OMC) of 15.5% and a maximum dry density (MDD) of 1.82 g/cm^3. Prior to use, the MLD soil was conditioned by oven drying at 40°C for at least 24 hours to minimize moisture.

The precursor selected for the study is ground granulated blast furnace slag (GGBS), supplied by VVM cement company in Belgium. Figure 1 displays the particle size distributions of both the GGBS and the MLD soil, while Table 1 reports their chemical compositions as determined by X-ray fluorescence (XRF) analysis. X-ray diffraction (XRD) analyses were performed on the raw MLD soil and on a mixture containing 5 wt% GGBS (referred to as SG). As shown in Figure 2, the predominant crystalline phases identified in both samples are quartz, muscovite, and albite, with minor amounts of microcline and clinochlore. The addition of GGBS did not result in the appearance of new crystalline phases, indicating its predominantly amorphous nature.

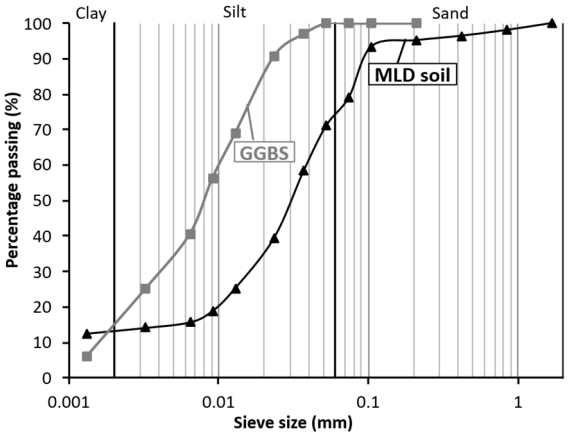

Figure 1. Particle size distribution curves of MLD soil and GGBS.

Sodium hydroxide (NaOH) solution was employed as the activator to promote the dissolution of the precursor. It was prepared in the laboratory by dissolving NaOH pellets (99% purity) in distilled water. The solution was afterwards maintained in a sealed container and kept in darkness for 24 hours before use, both to avoid degradation and to ensure the complete dissipation of heat generated during preparation.

Table 1. Chemical composition of GGBS and MLD.

Component (percentage by mass %)	MLD	GGBS
CaO	0.7	43.2
SiO_2	71.4	36.3
Al_2O_3	13.9	10.5
MgO	1.2	2.6
SO_3	0.02	1.5
K_2O	2.5	0.7
Fe_2O_3	4.3	0.6
TiO_2	0.9	0.5
Na_2O	0.8	0.2

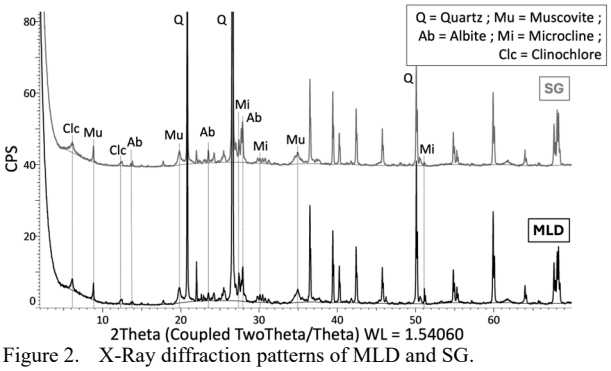

Figure 2. X-Ray diffraction patterns of MLD and SG.

2.2 *Mix proportions and sample manufacture*

To assess the influence of natural carbonation on the mechanical and microstructural behaviour of alkali-activated soils, three types of cylindrical specimens were produced: (i) reference samples made of untreated MLD soil (MLD), (ii) slag-stabilized samples composed of MLD soil and 5% GGBS mixed with distilled water (SG), and (iii) alkali-activated samples prepared with MLD soil, 5% GGBS, and a NaOH activator solution at 2M. The selected precursor content and activator concentration were established based on preliminary results on the same soil-precursor-activator system, seeking an optimal balance between compressive strength increase and the minimization of GGBS and NaOH consumption.

For each mixture, the quantity of solids was determined to achieve the target dry density, which was 1.82 g/cm^3 for untreated MLD and 1.79 g/cm^3 for stabilized mixtures. These values correspond to the maximum dry densities determined from the Standard Proctor compaction tests performed on both the MLD soil and the MLD + 5% GGBS blend. The initial water content during manufacturing was set to 15.5% for MLD soil and 16.5% for the stabilized mixtures, in line with the respective optimum moisture contents.

Sample preparation began with the manual homogenization of the dry components, namely MLD soil and GGBS (when applicable), until a uniform mix was obtained. The liquid phase, either distilled water or NaOH solution, was then gradually incorporated while mixing continued manually until the mixture reached a homogeneous and workable consistency. The prepared mixtures were then compacted into cylindrical molds of 36 mm in diameter and 72 mm in height in three equal layers and subsequently demolded using a hydraulic press. Curing was then carried out under two different environments:

- **Wrapped (WR)**: Samples were immediately wrapped in plastic film, aluminum foil and coated with paraffin to prevent any interaction with the ambient atmosphere and thus avoid CO_2 exposure. Samples were then stored under controlled laboratory conditions at a temperature of 19 ± 2°C and relative humidity of 40 ± 5%. Under these

conditions, only alkali-activation reactions are expected to occur.

- **Natural carbonation (OUT)**: Samples were placed outdoors in a sheltered area protected from external disturbances such as wind and rain. During the curing period, the temperatures were 16 ± 6°C, relative humidity averaged at 60 ± 20% and atmospheric CO_2 concentration was 0.04%. In this environment, both alkali-activation and natural carbonation processes are expected to take place.

MLD reference samples were only cured under wrapped conditions for 28 days, SG samples were cured under both wrapped and outside conditions for 28 days, and alkali-activated samples were cured under both conditions (WR and OUT) for 7 and 28 days.

2.3 *Mechanical testing and microstructural characterization*

Samples underwent unconfined compression tests (UCS) to assess their mechanical performance, specifically their unconfined compressive strength. The tests were conducted at a constant axial displacement rate of 0.06 mm/min, and testing continued until either sample failure occurred or an axial strain of 20% was reached, in accordance with ASTM D2166 standards (ASTM D2166, 2013). Three replicate specimens were tested for each curing condition. The water content at the time of testing was determined for each sample by weighing a representative portion before and after oven drying for 24 hours at 105 °C.

Mercury Intrusion Porosimetry (MIP) was then performed using an AutoPore IV 9500 (Micromeritics) to determine pore size distribution (3nm - 300µm) and total porosity. The technique measures mercury intrusion under increasing pressure, with pore diameters calculated via Washburn's equation. Prior to testing, samples were freeze-dried by rapid freezing in liquid nitrogen (−196 °C) and vacuum sublimation at −50 °C to preserve the microstructure.

Finally, X-ray diffraction (XRD) analyses were conducted using a Bruker D8 Advance Eco diffractometer equipped with a Cu Kα radiation source (WL = 1.5406 Å), operating at 40 kV and 25 mA. Data were collected over a 2θ range of 2°–70° with a step size of 0.019° and a counting time of 1 s per step. Before testing, samples were oven-dried at 105 °C for 24 h to remove residual moisture and subsequently ground into a fine powder using an agate mortar. The diffractograms were processed and analyzed with DIFFRAC.EVA software.

3 RESULTS AND DISCUSSIONS

3.1 *UCS*

Figure 3 shows results from the unconfined compression tests, with each data point corresponding to the average value obtained from three replicate and error bars indicating the standard deviation. The average water content measured at the time of testing is also reported for each sample type.

For the wrapped samples (WR), a progressive increase in unconfined compressive strength (UCS) is observed with both the addition of slag and longer curing durations. The incorporation of GGBS into the soil, without any chemical activation, already leads to a notable improvement in strength, doubling the UCS from 0.14 MPa (MLD) to 0.30 MPa (SG). This initial gain can be attributed to the fine particle size of GGBS, which enhances particle packing and contributes to the formation of a denser and mechanically stronger matrix. When combined with alkaline activation, strength development is

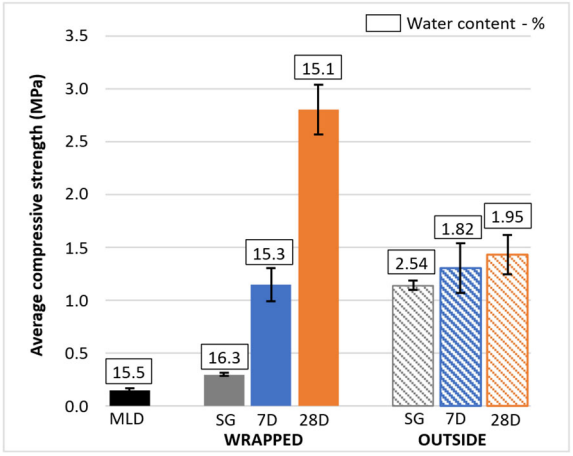

Figure 3. UCS results for all tested conditions.

further amplified due to the formation of aluminosilicate hydrate gels. These binding phases progressively form and densify over time, resulting in a significant increase in UCS from 1.15 MPa at 7 days to 2.80 MPa at 28 days. Besides, in unsaturated soils, a phenomenon called suction, which refers to the apparent forces between particles caused by capillary water in the pores is present. As water content decreases, suction increases, reinforcing interparticle bonds and enhancing mechanical strength. A general trend can thus be observed: the drier the sample, the higher the strength. Conversely, higher water content reduces suction and weakens the material (Jaquin et al., 2009; Bui et al., 2014). In this discussion, since all samples exhibit similar water contents, suction effects are expected to be comparable across the different conditions. Therefore, the observed differences in mechanical performance can be primarily attributed to the chemical and microstructural evolution induced by GGBS addition and alkaline-activation.

For samples cured in natural carbonation conditions (OUT), the strength trend contrasts with that observed for wrapped specimens. The unactivated slag-soil mixture (SG) shows a relatively high UCS of 1.14 MPa, which can be primarily attributed to its low water content (~2%). Since the mixture does not contain any alkaline activator (such as NaOH), the pH of the pore solution remains too low to allow significant CO_2 dissolution and reaction. As a result, carbonation is strongly limited in this case and the higher strength is most likely due to drying.

In contrast, alkali-activated samples cured outdoors for 7 and 28 days exhibit only a slight increase in strength (1.30 and 1.43 MPa, respectively), despite being chemically activated. This limited strength development suggests that the geopolymerization of aluminosilicate hydrate gels is strongly hindered under natural carbonation. One hypothesis is that atmospheric CO_2 interacts with available calcium ions in the slag or early-stage gels, favoring the formation of calcium carbonate over gel development. While this may contribute to the slight strength gain observed, the overall mechanical performance remains significantly lower than that of the corresponding wrapped samples, despite the OUT samples being drier. Furthermore, the lower water content of OUT samples likely reduces the availability of free water necessary for ion mobility, dissolution of precursors, and subsequent polymerization. As a result, even though partial carbonate formation may contribute to the slight gain observed, the overall mechanical performance remains significantly lower than in the corresponding wrapped samples. These results indicate that natural carbonation can significantly hinder the development of gels and compromise the effectiveness of the stabilization process.

3.2 *MIP*

Pore size distribution analysis was carried out on slag-stabilized samples (SG), on samples cured for 7 and 28 days under both OUT and WR conditions, as well as on an alkali-activated sample tested immediately after mixing (WR 0D), in order to assess the direct effect of NaOH addition on microstructural development (Figure 4 andFigure 5).

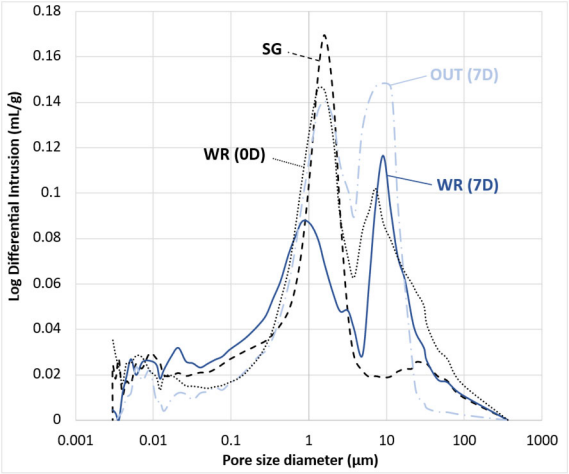

Figure 4. MIP results for 7d-cured and SG samples.

The SG sample, which contains no alkaline activator, exhibits a unimodal pore structure, with a dominant pore size ranging from 1 to 4 µm. In contrast, the WR 0D sample, tested immediately after alkali-activation, already displays a bimodal distribution, with a secondary family of larger pores between 5 and 12 µm. This shift reflects the immediate effect of the NaOH solution on the material fabric: the alkaline environment alters the electrochemical balance at particle edges, increasing interparticle repulsion and causing structural dispersion, which generates macropores (Chavali et al., 2017; Barakat et al., 2024). After 7 days of curing (Figure 4), both WR and OUT samples continue to show bimodal distributions, with two distinguishable pore families in similar pore size ranges. Notably, the relative intensity of the macropore peak becomes more pronounced, suggesting ongoing microstructural rearrangement. By 28 days (Figure 5), the pore structure shows a further shift, where the macropore family becomes the dominant one, with the second peak clearly exceeding the first in intensity. This evolution highlights a progressive reorganization of the pore network, likely driven by the formation of new phases (alkali activation gels but also calcium carbonate) and matrix densification, resulting in a redistribution

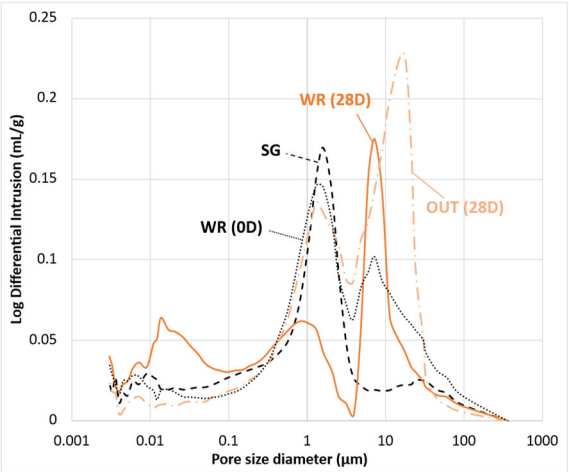

Figure 5. MIP results for 28d-cured samples and SG samples.

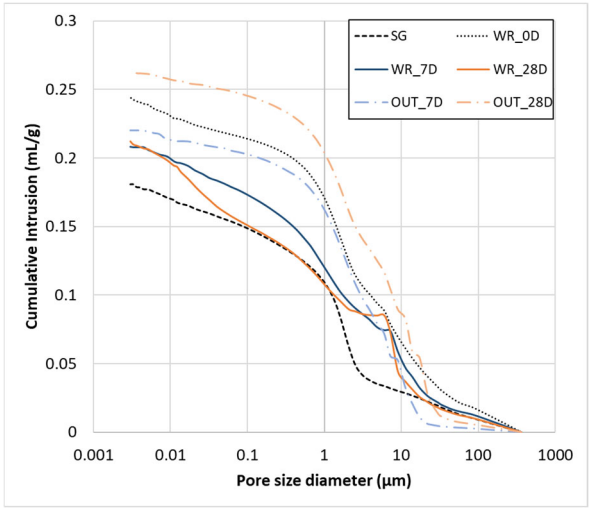

Figure 6. Cumulative intrusion for MIP tests.

of pore sizes and connectivity.

Cumulative intrusion data (Figure 6) corroborates these trends. The WR 0D sample exhibits a higher total intruded volume than SG, confirming that the alkaline environment rapidly induces structural dispersion and macropore formation after NaOH addition. Upon curing, WR samples show a marked reduction in total pore volume at both 7 and 28 days, indicating progressive gel precipitation and pore filling, which reduce overall porosity. On the other hand, OUT samples display only a slight decrease in volume at 7 days, consistent with the onset of gel formation, but show a significant increase at 28 days. This increase is likely linked to carbonation processes, where calcite precipitation by gel decalcification causes volume expansion and the formation of macropores (Lamaa et al., 2023).

3.3 *XRD*

Figures 7 and 8 show the X-ray diffraction (XRD) patterns of the untreated soil (MLD) alongside the alkali-activated samples cured for 7 and 28 days under wrapped (WR) and natural carbonation (OUT) conditions, respectively. In all cases, the dominant crystalline phases, namely quartz, muscovite, and albite are still clearly identifiable, which is expected given their chemical and structural stability throughout the alkali-activation process.

In the WR samples, XRD patterns reveal the presence of a new crystalline phase, gismondine, which is a zeolitic aluminosilicate commonly associated with alkali-activation processes (Bernal et al., 2012; Marsh et al., 2019a). Its presence supports the formation of CASH gels. Although these gels are predominantly amorphous and thus not directly detectable by XRD, the detection of gismondine as a crystalline secondary product may serve as an indirect indicator of their formation. Additionally, the characteristic peaks of clinochlore disappear after alkali-activation, indicating partial dissolution of this mineral under alkaline conditions. While this highlights the potential reactivity of certain soil minerals, the primary source of reactive calcium, silica and alumina for the gel formation remains the amorphous GGBS precursor.

In the OUT samples, a small amount of gismondine is detected at 7 days, though less clearly than in the corresponding WR samples. By 28 days, this phase becomes less apparent or even absent, which could be attributed to decalcification due to carbonation, or possibly to the limited stability of the mineral over time. As in the WR samples, the disappearance of clinochlore peaks indicates its partial dissolution in the alkaline environment. Notably, calcite is detected at 28 days, confirming

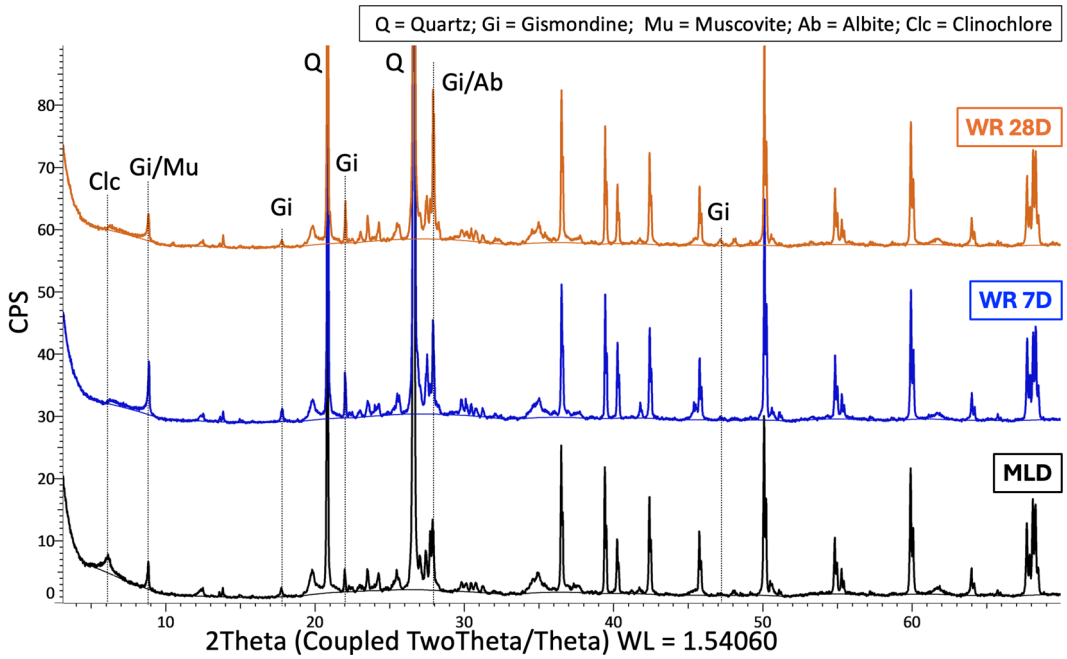

Figure 7. X-ray diffraction patterns of MLD soil and wrapped samples.

that carbonation has occurred during curing under ambient conditions. These findings highlight a clear correlation between the microstructural evolution observed through XRD and the mechanical performance measured by UCS tests. In wrapped conditions, the detection of gismondine supports the progressive development of amorphous binding phases, consistent with the significant strength gain over time.

Conversely, under natural carbonation, the limited formation of gismondine, the presence of calcite, and the moderate strength increase suggest that carbonation processes partially inhibit gel formation, ultimately compromising the effectiveness of alkali-activation.

4 CONCLUSION

This study investigated the influence of natural carbonation on the mechanical and microstructural development of alkali-activated fine-grained soils. Sealed curing promoted the progressive formation of CASH gels, resulting in significant strength gains and pore structure densification. Under natural carbonation, however, strength development was limited despite lower water contents, with XRD and MIP analyses revealing reduced gel formation, calcite precipitation, and possible gel decalcification.

These findings demonstrate that natural carbonation can compete with alkali-activation reactions, compromising stabilization efficiency. The study provides valuable insights into the impact of natural carbonation on alkali-activated soil stabilization, a key factor for predicting in-service performance and durability in geotechnical engineering.

Future research should explore the influence of precursor composition, particularly with lower calcium contents, assess the effect of curing sequence and protocols, and apply complementary techniques such as thermogravimetric analysis (TGA) or Fourier Transform Infrared Spectroscopy (FTIR) to better characterize gel chemistry and calcium carbonate formation.

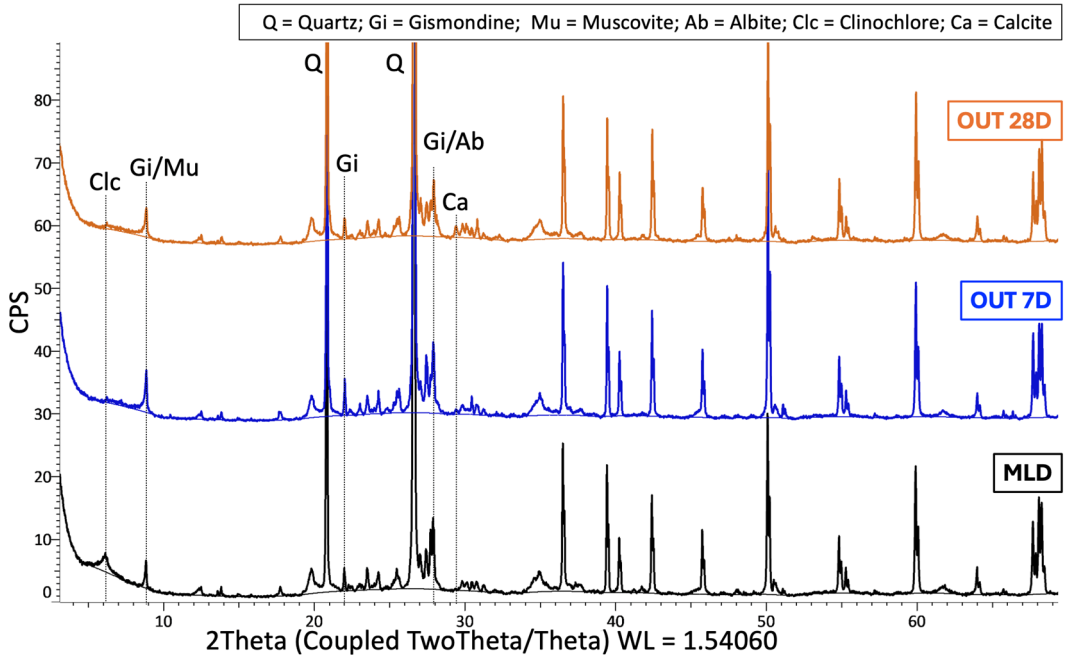

Figure 8. X-ray diffraction patterns of MLD and carbonated samples cured outside.

5 REFERENCES

American Society for Testing and Materials International, 2021. *ASTM D698, Standard Test Methods for Laboratory Compaction Characteristics of Soil Using Standard Effort (12.400 ft-lbf/ft3 (600 kN-m/m3))*.

Anon. n.d. *siva-classification.pdf*. Available at: <https://www.geoengineer.org/storage/education/10/general_file_collection/7906/siva-classification.pdf> [Accessed 26 March 2025].

American Society for Testing and Materials International, 2017. *ASTM D 4318-17E01*, *Standard Test Methods for Liquid Limit, Plastic Limit, and Plasticity Index of Soils.*

American Society for Testing and Materials International, 2013. *ASTM D2166, Standard Test Method for Unconfined Compressive Strength of Cohesive Soil.*

Barakat, Y., Mokni, N., Cui, Y.-J. and Bernier, F., 2024. Effects of Salinity and Alkalinity on the Volumetric Deformation of the Opalinus Clay from the Lower Sandy Facies (LSF) of Mont Terri Site. *Rock Mechanics and Rock Engineering*, 57(11), pp.9251–9273. https://doi.org/10.1007/s00603-024-04028-9.

Bernal, S.A., Provis, J.L., Brice, D.G., Kilcullen, A., Duxson, P. and van Deventer, J.S.J., 2012. Accelerated carbonation testing of alkali-activated binders significantly underestimates service life: The role of pore solution chemistry. *Cement and Concrete Research*, 42(10), pp.1317–1326. https://doi.org/10.1016/j.cemconres.2012.07.002.

Bui, Q.-B., Morel, J.-C., Hans, S. and Walker, P., 2014. Effect of moisture content on the mechanical characteristics of rammed earth. *Construction and Building Materials*, 54, pp.163–169. https://doi.org/10.1016/j.conbuildmat.2013.12.067.

Chavali, R.V.P., Vindula, S.K., P, H.P.R., Babu, A. and Pillai, R.J., 2017. Swelling behavior of kaolinitic clays contaminated with alkali solutions: A micro-level study. *Applied Clay Science*, 135, pp.575–582. https://doi.org/10.1016/j.clay.2016.10.045.

Cristelo, N., Glendinning, S., Fernandes, L. and Pinto, A.T., 2012. Effect of calcium content on soil stabilisation with alkaline activation. *Construction and Building Materials*, 29, pp.167–174. https://doi.org/10.1016/j.conbuildmat.2011.10.049.

Cui, Y., Li, H., Zhang, S. and Li, L., 2025. Sequential alkali activation and carbonation synergy: Optimized valorization of steel slag soil blocks. *Materials Today Communications*, 47, p.113149. https://doi.org/10.1016/j.mtcomm.2025.113149.

Fasihnikoutalab Mohammad Hamed, Asadi Afshin, Unluer Cise, Huat Bujang Kim, Ball Richard J., and Pourakbar Shahram, 2017. Utilization of Alkali-Activated Olivine in Soil Stabilization and the Effect of Carbonation on Unconfined Compressive Strength and Microstructure. *Journal of Materials in Civil Engineering*, 29(6), p.06017002. https://doi.org/10.1061/(ASCE)MT.1943-5533.0001833.

Jaquin, P., Augarde, C., Gallipoli, D. and Toll, D., 2009. The strength of unstabilised rammed earth materials. *Géotechnique*, 59, pp.487–490. https://doi.org/10.1680/geot.2007.00129.

Ko, M.-S., Chen, Y.-L. and Jiang, J.-H., 2015. Accelerated carbonation of basic oxygen furnace slag and the effects on its mechanical properties. *Construction and Building Materials*, 98, pp.286–293. https://doi.org/10.1016/j.conbuildmat.2015.08.051.

Lamaa, G., Duarte, A.P.C., Silva, R.V. and de Brito, J., 2023. Carbonation of Alkali-Activated Materials: A Review. *Materials*, 16(8). https://doi.org/10.3390/ma16083086.

Li, L. and Wu, M., 2022. An overview of utilizing CO2 for accelerated carbonation treatment in the concrete industry. *Journal of CO2 Utilization*, 60, p.102000. https://doi.org/10.1016/j.jcou.2022.102000.

Marsh, A., Heath, A., Patureau, P., Evernden, M. and Walker, P., 2019a. Phase formation behaviour in alkali activation of clay mixtures. *Applied Clay Science*, 175, pp.10–21. https://doi.org/10.1016/j.clay.2019.03.037.

Marsh, A., Heath, A., Patureau, P., Evernden, P. and Walker, P., 2019b. Influence of clay minerals and associated minerals in alkali activation of soils. *Construction and Building Materials*, 229, p.116816. https://doi.org/10.1016/j.conbuildmat.2019.116816.

Mavroulidou, M., Gray, C., Gunn, M.J. and Pantoja-Muñoz, L., 2022. A Study of Innovative Alkali-Activated Binders for Soil Stabilisation in the Context of Engineering Sustainability and Circular Economy. *Circular Economy and Sustainability*, 2(4), pp.1627–1651. https://doi.org/10.1007/s43615-021-00112-2.

Mazhar, S., GuhaRay, A., Kar, A., Avinash, G.S.S. and Sirupa, R., 2018. Stabilization of Expansive Black Cotton Soils with Alkali Activated Binders. In: W. Wu and H.-S. Yu, eds. *Proceedings of China-Europe Conference on Geotechnical Engineering*. Cham: Springer International Publishing. pp.826–829.

Miraki, H., Shariatmadari, N., Ghadir, P., Jahandari, S., Tao, Z. and Siddique, R., 2022. Clayey soil stabilization using alkali-activated volcanic ash and slag. *Journal of Rock Mechanics and Geotechnical Engineering*, 14(2), pp.576–591. https://doi.org/10.1016/j.jrmge.2021.08.012.

Murmu, A.L., Jain, A. and Patel, A., 2019. Mechanical Properties of Alkali Activated Fly Ash Geopolymer Stabilized Expansive Clay. *KSCE Journal of Civil Engineering*, 23(9), pp.3875–3888. https://doi.org/10.1007/s12205-019-2251-z.

Polettini, A., Pomi, R. and Stramazzo, A., 2016. CO2 sequestration through aqueous accelerated carbonation of BOF slag: A factorial study of parameters effects. *Journal of Environmental Management*, 167, pp.185–195. https://doi.org/10.1016/j.jenvman.2015.11.042.

Razeghi, H.R., Safaee, F., Geranghadr, A., Ghadir, P. and Javadi, A.A., 2024. Investigating accelerated carbonation for alkali activated slag stabilized sandy soil. *Geotechnical and Geological Engineering*, 42(1), pp.575–592. https://doi.org/10.1007/s10706-023-02590-7.

Tonini De Araújo, M., Tonatto Ferrazzo, S., Mansur Chaves, H., Gravina Da Rocha, C. and Cesar Consoli, N., 2023. Mechanical behavior, mineralogy, and microstructure of alkali-activated wastes-based binder for a clayey soil stabilization. *Construction and Building Materials*, 362, p.129757. https://doi.org/10.1016/j.conbuildmat.2022.129757.

Vitale, E., Russo, G., Dell'Agli, G., Ferone, C. and Bartolomeo, C., 2017. Mechanical Behaviour of Soil Improved by Alkali Activated Binders. *Environments*, 4(4). https://doi.org/10.3390/environments4040080.